Rapid Communications

Successive electric-polarization switches in the $S = 1/2$ skew chain $Co_2V_2O_7$ induced by a high magnetic field

R. Chen,[1] J. F. Wang,[1,*] Z. W. Ouyang,[1,†] M. Tokunaga,[2] A. Y. Luo,[1] L. Lin,[3] J. M. Liu,[3] Y. Xiao,[4] A. Miyake,[2] Y. Kohama,[2] C. L. Lu,[1] M. Yang,[1] Z. C. Xia,[1] K. Kindo,[2] and L. Li[1]

[1]*Wuhan National High Magnetic Field Center and School of Physics, Huazhong University of Science and Technology, Wuhan 430074, China*

[2]*The Institute for Solid State Physics (ISSP), University of Tokyo, Chiba 277-8581, Japan*

[3]*Laboratory of Solid State Microstructures and Innovative Center of Advanced Microstructures, Nanjing University, Nanjing 210093, China*

[4]*School of Advanced Materials, Peking University Shenzhen Graduate School, Shenzhen 518055, China*

(Received 16 July 2019; revised manuscript received 19 September 2019; published 7 October 2019)

We report successive electric-polarization (P) switches in the $S = 1/2$ quantum magnet $Co_2V_2O_7$ by application of a magnetic field along the b axis, where a 1/2-magnetization plateau is seen at 5.4–11.6 T. Polarization reversal appears at ~5 T from $-P \parallel b$ to $+P \parallel b$, leading to an irreversible magnetoelectric history involved with a memory effect, while the polarization flop in fields of 12–17 T is identified by a transition from the $P \parallel b$ to $P \parallel ac$ plane, different from those reported previously. These intriguing magnetoelectric phenomena are owing to the unique nature of the skew-chain-like magnetic structure of $Co_2V_2O_7$ and can be understood by a change in symmetry of the magnetic order in applied fields. The emergent ferroelectricities deviating from the half-plateau state may arise from magnon Bose-Einstein condensation in this quantum magnet.

DOI: 10.1103/PhysRevB.100.140403

The magnetic control of ferroelectricity becomes a key subject of multiferroic materials since the discovery of a gigantic magnetoelectric response in rare-earth perovskite manganites [1–3]. Intriguing phenomena of this effect are known as the electric-polarization (P) flop (90°) observed in $RMnO_3$ (R = Tb, Dy) and RMn_2O_5 (R = Tm, Yb) [1,3–7], and P reversal (180°) as observed in $TbMn_2O_5$ by application of a magnetic field (H) [2]. Polarization flops were found in other magnetically induced multiferroic materials such as the spin-chain cuprate $LiCu_2O_2$ and huebnerite $MnWO_4$ [8,9]. In these materials, the produced ferroelectricity can be described by the inverse Dzyaloshinskii-Moriya (or spin current) mechanism [10], i.e., $P \propto e_{ij} \times (S_i \times S_j)$, where e_{ij} is a vector that connects the spins S_i and S_j. Thus the P direction is connected to the vector chirality $C(= S_i \times S_j)$ of the spiral spin structure [11,12]. A recent optical study on $TbMnO_3$ revealed the deterministic nature of the P flop with a unique correspondence [13]. So far, the microscopic origin and the magnetic structure of the flopped ferroelectric (FE) phase in these systems still remain puzzling [14–16]. On the other hand, polarization reversal also arouses considerable interest. Different from the normal manipulation of P by a reversal of H [17,18], it can be obtained unexpectedly by extending H to higher fields without bias electric fields [2,19–23]. Furthermore, P reversals are also realized in $TbMnO_3$ or $MnWO_4$ through rotating the H direction in a peculiar crystallographic plane, in which magnetoelectric memory plays an important role in the process [24,25].

In general, polarization flop and reversal do not take place in the same field direction. For instance, $MnWO_4$ exhibits the P-flop transition for $H \parallel b$ [9], while P reversal occurs when H is applied along the magnetic easy axis [20] or rotated from $+a$ to b to $-a$ [25]. In this Rapid Communication, we report an observation of successive polarization switches (reversal and flop) in an $S = 1/2$ skew-chain vanadate $Co_2V_2O_7$. We identify that the b-axis field induces a P reversal at ~5 T and then a paraelectric state at 5.4–11.6 T followed by a P flop at 12–17 T from the b axis to the ac plane. This unusual flop of a reentrant FE state is certainly different from the P flops of spontaneous ferroelectricity as reported previously. These experimental findings, reminiscent of polarization switching by application of a large magnetic field in $Co_2V_2O_7$, help to establish a close correlation between these two nontrivial magnetoelectric phenomena.

Recently, $Co_2V_2O_7$ has received increased attention because of its exotic properties such as the quantum magnetization (M) plateau and multiferroic behaviors [26,27]. This compound crystallizes in a monoclinic structure (space group $P2_1/c$) as shown in Fig. 1(a). The angle β between a and c is 100.12° while b is normal to the ac plane. Two nonequivalent Co^{2+} spins form bond-alternating skew chains along c which are separated by nonmagnetic tetrahedrons VO_4 between the chains. When temperature (T) is reduced below $T_N = 6.3$ K, $Co_2V_2O_7$ undergoes antiferromagnetic ordering mainly along the b axis, where the Co^{2+} spins behave as effective $S = 1/2$ spins [27]. Unlike the isostructural $Ni_2V_2O_7$ [28], $Co_2V_2O_7$ shows a large interchain coupling resulting in an anisotropic 1/2-magnetization plateau at 5.4–11.6 T only for $H \parallel b$ [27]. A previous study using a polycrystalline sample revealed H-induced ferroelectricity and magnetoelectric coupling below T_N [26]. The frustration factor estimated from the susceptibility data is $\theta_p/T_N \sim 3$, with θ_p the Weiss constant, indicating a weak magnetic frustration in $Co_2V_2O_7$.

*jfwang@hust.edu.cn
†zwouyang@mail.hust.edu.cn

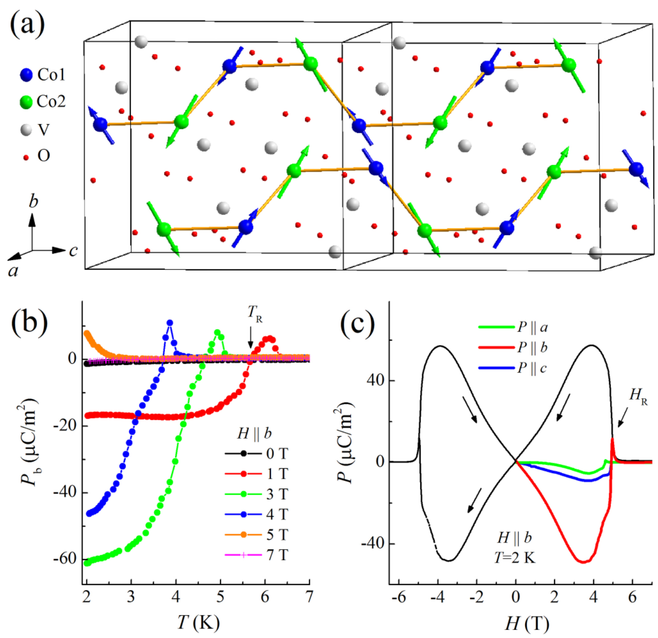

FIG. 1. (a) Crystal and magnetic structures of $Co_2V_2O_7$ in the ground state as reported in Ref. [37]. (b) T dependence of P_b in fields of 0–7 T. P was measured upon warming at a rate of 4 K/min. T_R is the transition temperature of P_b from positive to negative. (c) H dependence of P_a, P_b, and P_c, respectively. The sample was cooled down through the Néel temperature under a poling field of 650 kV/m, which was removed at 2 K and then the pyroelectric current was measured for (b) and (c), respectively. H_R denotes the transition field of P_b from negative to positive. The black curve denotes a measurement of P_b with scanning of H between ±7 T.

Single crystals of $Co_2V_2O_7$ were grown using V_2O_5 as self-flux [29]. The crystals are oriented and cut into thin plates with dimensions of $\sim 1 \times 1 \times 0.2\,mm^3$. The low-field electric polarization was measured based on a physical properties measurement system (PPMS) by probing the zero-electric-field pyroelectric current. High-field magnetization and electric polarization were measured using a 10.5-ms short-pulse magnet in the Wuhan National High Magnetic Field Center (WHMFC). A high-field dielectric constant was measured using a capacitance bridge in the International MegaGauss Science Laboratory of the ISSP at the University of Tokyo.

We focus on the magnetic field direction along b where a quantum plateau in M appears in a high field. Figure 1(b) shows the temperature dependence of P_b ($P \parallel b$) in various fields. At $H = 0$ T, no polarization is observed, suggestive of a paraelectric ground state. At a field of 1 T, however, a finite P appears below T_N and changes its sign from positive to negative at T_R. As H increases, T_R moves to low T and vanishes at $H = 5$ T. The positive P is $\sim 10\,\mu C/m^2$ but the negative P has a maximum magnitude of $60\,\mu C/m^2$ at $H = 3$ T. At $H = 7$ T, P vanishes completely, indicating the system enters a new paraelectric phase. Figure 1(c) shows the variations of P with different directions as a function of H. As H increases, P_b varies from zero to negative and reaches a minimum value of $-50\,\mu C/m^2$ at 3 T. By contrast, there is only a tiny signal for P_a and P_c possibly due to a misalignment of the crystal. This means the H-induced P mainly orients along the b axis. Another observation is the sign reversal of P_b at $H_R = 5$ T. In a higher field, P_b returns to zero quickly up to 7 T. This $P_b(H)$ behavior is consistent with the $P_b(T)$ data in Fig. 1(b). We further scan H between ±7 T (the black curve). As H decreases, surprisingly, P_b does not follow the trace of the H-increasing process but remains positive from H_R to 0 T. The P reversal is also seen in a negative H scanning. This irreversible history dependence of P and its reversal [also see Fig. S1 of the Supplemental Material (SM) [30]] are distinct from those reported previously [2,17–25], evidenced as a unique polarization reversal in $Co_2V_2O_7$. A similar butterfly-type profile of the magnetoelectric response was previously reported in $Ni_3B_7O_{13}I$ [31], in which ferroelectricity and weak ferromagnetism were found due to the time-reversal symmetry breaking. In the case of $Co_2V_2O_7$, however, no weak ferromagnetism is found. In addition, the butterfly curve shown in Fig. 1(c) takes a negative P path when the $+H$ increases, different from the result for $Ni_3B_7O_{13}I$ [31]. It looks even for time-reversal symmetry that P_b just below the plateau state is always positive for ±7 T. We attribute this phenomenon to a magnetoelectric memory effect, namely, the information of the P direction and the spin chirality are memorized in the paraelectric 1/2-plateau phase and read out in the H-decreasing process. This memory effect, associated with the P reversal as observed in $MnWO_4$ and $Ni_3V_2O_8$, can be driven either thermally or magnetically [25,32], also consistent with the observations in Figs. 1(b) and 1(c).

Figure 2(a) presents the magnetization of $Co_2V_2O_7$ in a pulsed field to 28 T. After a steep increase below ∼5 T, the M shows a half plateau between $H_{P1} = 5.4$ T and $H_{P2} = 11.6$ T. This anisotropic quantum plateau was explained by a collinear "↑↑↑↓" spin arrangement as proposed by Yin *et al.* [27]. More transitions are seen at $H_R = 5$ T, $H_F = 14.6$ T, and $H_S = 18.5$ T in the derivative dM/dH. Figures 2(b)–2(d) display the field dependences ($H \parallel b$) of the dielectric constant (ε), pyroelectric current (I), and P with electrodes along different directions. Pronounced magnetoelectric responses are observed at magnetic transitions of H_R-H_S. At H_R, ε_b shows a large magnetocapacitance with a change of $\Delta\varepsilon/\varepsilon(0) \sim 40\%$, corresponding to a change of I_b and suppression of P_b at this transition. In the polarization measurements under pulsed fields, we applied bias electric fields of 1 MV/m to sufficiently polarize the domains. Thus the unusual P reversal in Fig. 1(c) is not reproduced in the data of Fig. 2(d). The most important finding in Fig. 2(d) is given by the H-induced electric polarizations between H_{P2} and H_S, i.e., P_b (P_a, P_c) centered at H_{P2} - H_F(H_F-H_S). These emergent ferroelectricities are also characterized by the variations of ε and I as shown in Figs. 2(b) and 2(c). Since $b \perp ac$ plane, this magnetic switch of P in a high field can be regarded as a polarization flop from the b axis to a direction in the ac plane. From the amplitude values of P_a and P_c, we estimate that the direction of the flopped P deviates from the c axis with an angle of $\sim 30^\circ$.

Figure 3(a) shows the profiles of $P_a(H)$-$P_c(H)$ measured in various temperatures (see Fig. S2 of SM in a large field range [30]), in which the polarization flop in $Co_2V_2O_7$ is well established. Through comprehensive measurements, we construct the H-T phase diagram of $Co_2V_2O_7$ in Fig. 3(b), where a polarization flop (FE-II → FE-III) and reversal (FE-I→FE-I′) are both included. Compared with the P flops

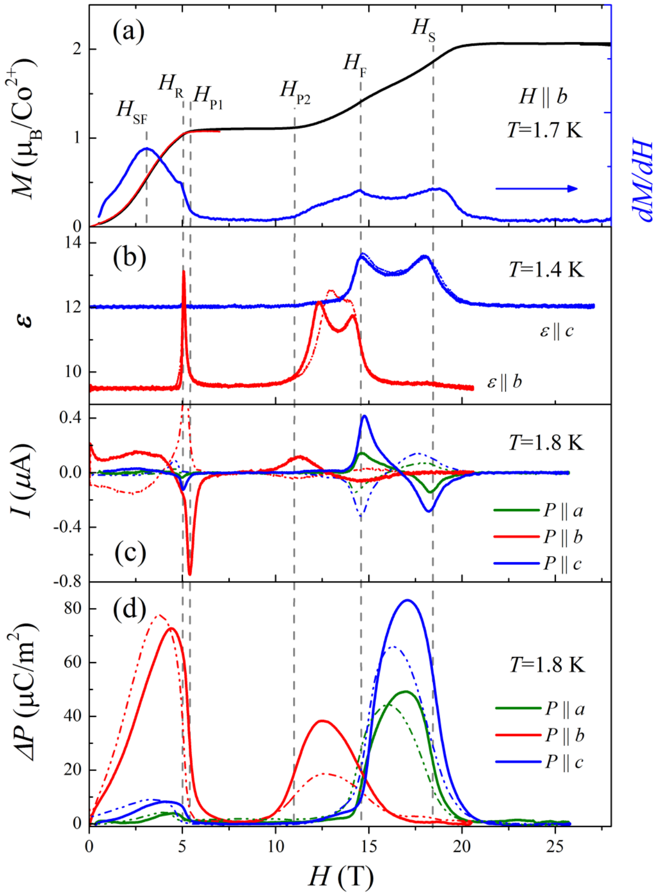

FIG. 2. Magnetic field ($H \parallel b$) variations of (a) M and the derivative dM/dH measured at 1.7 K. M is corrected for Van Vleck paramagnetism, (b) the dielectric constant ε at 1.4 K for $\varepsilon \parallel b$ and $\varepsilon \parallel c$ at a frequency of 50 kHz, and (c), (d) the pyroelectric current I and the integrated P at 1.8 K for electrodes along a, b, and c, respectively. The red curve is calibrated data in a dc field. The sample was cooled down under an electric field of 1 MV/m, which was maintained during the pulse to fully polarize the H-induced FE domains. Solid (dashed-dotted) lines in (b)–(d) represent the field-rising (falling) sweeps. Dashed lines in (a)–(d) show the transition fields of H_{SF}-H_S.

reported previously [1,3–9], the present study shows several distinct differences: First, it takes place at a reentrant FE state, not as spontaneous ferroelectricity, and the flopped direction is not along a crystallographic axis as reported. Second, earlier studies revealed that the P flop is strongly temperature dependent [6–8,33,34], but it is nearly independent with the temperature in $Co_2V_2O_7$. The transition field ($H_F \sim 15$ T) is also much higher than 0.5–3 T as reported for the manganites and $LiCu_2O_2$. Third, the flops of P in $TbMnO_3$ and $MnWO_4$ coincide with a first-order transition from an incommensurate to a commensurate phase [1,9,35]. This manifested as a hysteresis in susceptibility or magnetization. Generally, this hysteresis of M becomes large in a pulsed field due to its fast sweeping rate. However, our magnetization data [27] do not show hysteresis across the P-flop transition, indicative of the nature of a second-order phase transition. These experimental findings suggest that the P flop of $Co_2V_2O_7$ observed in the b-axis field of 12–17 T is likely another type of polarization flop.

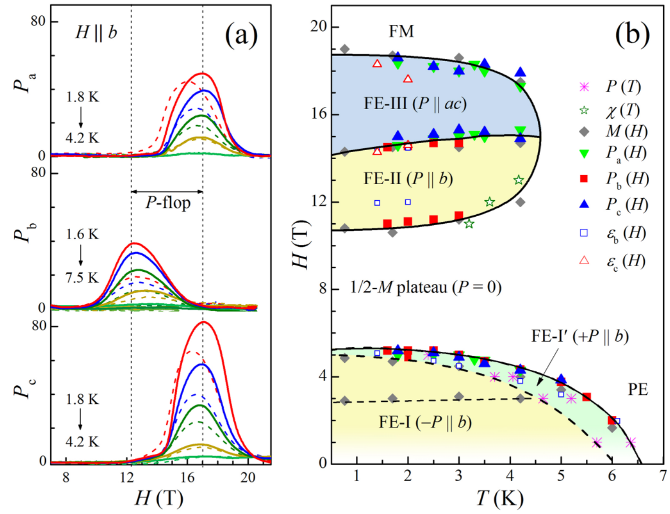

FIG. 3. (a) Field profiles of P_a-P_c in various temperatures. Vertical lines mark the field range of the P flop. Solid (dashed) lines indicate the H-rising (falling) sweeps. (b) The explored FE phases (FE-I, FE-I′, FE-II, and FE-III) and the phase diagram determined in this study. The gray dashed line in phase FE-I shows the spin-flop transition.

Normally, electric-polarization flop takes place in classical spin systems, for example, the perovskite manganites and $MnWO_4$ [1,3–7,9]. In these materials, the polarization flop was attributed to H-induced changes of the magnetic structure and vector chirality $C(= S_i \times S_j)$ [4,12,14]. Experimentally, this was verified in $TmMn_2O_5$ [6] and $DyMnO_3$ [33] from one cycloidal plane to another. However, it is hard to understand that such a classical picture of P flop can be applicable to the effective spin-1/2 system. On the other hand, it is difficult to reveal the magnetic structure of the flopped FE-III phase by means of a neutron diffraction measurement in such a high magnetic field. We notice that the b-axis magnetization at the flop transition is ∼3/4 of the total magnetic moments [27]. Usually, an umbrellalike spin structure often appears before the saturation magnetization. These facts rule out a simple ac-cycloidal spin structure of phase FE-III. Theoretically, a Monte Carlo analysis on the $S = 1/2$ kagome staircase $PbCu_3TeO_7$ also proposed a transverse conical spin order in the flopped $P \parallel c$ phase [36]. Whether or not the FE-III phase in Fig. 3(b) has a conical structure depends on the Dzyaloshinskii-Moriya vector of the material, which is unknown at present.

A FE phase transition of one material is usually the result of a broken symmetry from a parent phase to a FE phase accompanying the decrease of symmetry. As for $Co_2V_2O_7$, all the FE phases can be obtained by a second-order transition from the paraelectric ground state. Therefore, space groups of these phases can be derived from the parent one, i.e., $P2_1/c$ (No. 14). If c-glide symmetry is lost, it will be a polar crystal with $P \parallel b$ ($P2_1$, No. 4), while loss of twofold helical symmetry results in another polar crystal with $P \parallel ac$ (Pc, No. 7). Recently, the magnetic ground state of $Co_2V_2O_7$ was determined by our time-of-flight neutron powder diffraction experiment [37]. As illustrated in Fig. 1(a), $Co_2V_2O_7$ has a commensurate noncollinear spin structure in $H = 0$ T. For the Co1 site, $m_x = -0.26(5)\mu_B$, $m_y = 1.77(5)\mu_B$, $m_z = 0.97(5)\mu_B$; for the Co2 site, $m_x = 0.35(5)\mu_B$, $m_y = 2.38(5)\mu_B$, $m_z = 1.27(5)\mu_B$. All the Co^{2+} spins are antiferromagnetic ordered mainly in the *bc* plane and run along the *c* axis with a canted angle of 26°. The spin arrangement in Fig. 1(a) may not break the *c*-glide symmetry. But tilting of the magnetic moments toward the *b* axis by applied *H* will break it. Then the system becomes a polar crystal with space group $P2_1$. Note that this is a chiral space group, thus the polarization reversal from the FE-I to FE-I′ phase is correlated with the spin chirality as expected. The *P*-flop transition from the FE-II to FE-III phase corresponds to a change in symmetry from $P2_1$ to *Pc* in a higher field. For the flopped phase, *c*-glide symmetry is preserved while twofold helical symmetry is lost. If both of them are lost, the system possesses the space-reversal symmetry ($P\bar{1}$, No. 2). Consequently, ferroelectricity disappears, in agreement with $P = 0$ in the 1/2-*M* plateau phase. Thus, our symmetry analysis qualitatively explains the intriguing magnetoelectric phenomena in $Co_2V_2O_7$ in the $H \parallel b$ field.

Flop of the electric polarization is sometimes observed in the system that shows spin-induced polarization by the spin current mechanism, or equivalently by the inverse effect of the Dzyaloshinskii-Moriya interaction. In this mechanism, electric polarization is proportional to the vector spin chirality of the adjacent spins, i.e., $S_i \times S_j$, which can be transformed into the following formula using ladder operators,

$$(S_i \times S_j)_z = \left(\frac{i}{2}\right)(S_i^+ S_j^- - S_i^- S_j^+). \quad (1)$$

As is widely recognized for quantum magnets, the magnetization plateau state corresponds to a Mott insulator of magnetic excitation. Therefore, the existence of a gap in magnetic excitation is expected to suppress the spin current, which appears as the suppression of P_b in the present material. Such a quantum picture of a spin current mechanism is also utilized to explain spin-induced electric polarization in the magnon Bose-Einstein condensation state of $TlCuCl_3$ [38].

Figure 4 shows control of the polarization flop in $Co_2V_2O_7$ via rotating the *H* direction in the *bc* plane. For $0° < \theta < 30°$, phase FE-I is almost not changed. As θ is increased, by contrast, phase FE-II is suppressed, meanwhile phase FE-III is largely enhanced. When θ is about the canted angle of 26° in Fig. 1(a), the phenomenon of *P* flop disappears eventually. Similar behavior is observed for $-30° < \theta < 0°$ (not shown). This angular-dependent property indicates that the skew-chain-like crystal and magnetic structures play a crucial role for the polarization flop in $Co_2V_2O_7$. When θ is further increased, both low- and high-field FE phases evolve in an unusual way, where polarization reversals are found even under the application of an opposite bias electric field. This *P* reversal emerges when low- and high-field FE phases are converged for $\theta > 60°$. At $\theta = 90°$, a butterfly profile (P_c) is observed similar to the one seen in Fig. 1(c). Indeed, a small

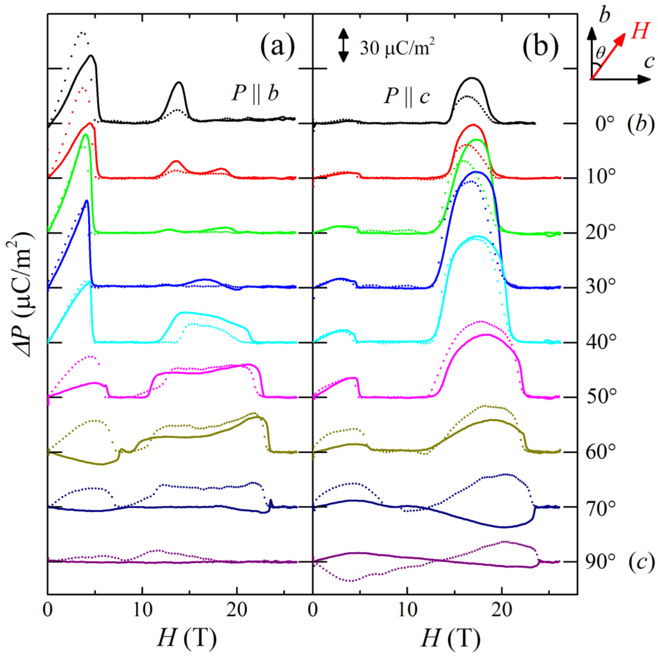

FIG. 4. Electric-polarization flop and reversal of $Co_2V_2O_7$ studied by rotating the *H* direction from the *b* to the *c* axis. (a), (b) show the evolutions of P_b and P_c measured at 1.8 K, respectively. θ is defined to be the angle between *b* and *H*. Solid (dotted) lines indicate the field-rising (falling) sweeps.

sign reversal of *P* at $P = 0$ is accompanied by the observed irreversible phenomenon with decreasing fields. Although the mechanism is unclear at this moment, these observations provide clues to understand the long-standing issue of polarization reversals in $MnWO_4$ [20,22] and $TbMn_2O_5$ [2], and the correlation between the polarization reversal and flop in the spin-spiral multiferroic materials.

To conclude, we have studied the ferroelectric polarization of $Co_2V_2O_7$ single crystals in magnetic fields applied along the *b* axis and observed electric-polarization reversal at ∼5 T and another flop in fields of 12–17 T. The half-plateau state between the *P* reversal and flop is likely a kind of Mott insulator of magnons in the framework of a quantum mechanism. We attribute these intriguing phenomena to a result of the peculiar skew-chain-like crystal and magnetic structures of $Co_2V_2O_7$ in applied magnetic fields. Further adequate experiments such as neutron diffraction under sufficient high fields are desirable to understand the magnetic structure of each ordered phase and the interesting observations in our angular study.

J.F.W. would like to thank S.-W. Cheong at Rutgers University for useful discussions. This work was supported by the NSFC of China (11574098, 11874023, U1832214, 51721001, and 11774106), the Fundamental Research Funds for the Central Universities (2018KFYXKJC005), and the National Key R&D Program of China (2016YFA0401704).

[1] T. Kimura, T. Goto, H. Shintani, K. Ishizaka, T. Arima, and Y. Tokura, Nature (London) **426**, 55 (2003).

[2] N. Hur, S. Park, P. A. Sharma, J. S. Ahn, S. Guha, and S. W. Cheong, Nature (London) **429**, 392 (2004).

[3] S.-W. Cheong and M. Mostovoy, Nat. Mater. **6**, 13 (2007).
[4] N. Aliouane, K. Schmalzl, D. Senff, A. Maljuk, K. Prokeš, M. Braden, and D. N. Argyriou, Phys. Rev. Lett. **102**, 207205 (2009).
[5] T. Goto, T. Kimura, G. Lawes, A. P. Ramirez, and Y. Tokura, Phys. Rev. Lett. **92**, 257201 (2004).
[6] M. Fukunaga, Y. Sakamoto, H. Kimura, Y. Noda, N. Abe, K. Taniguchi, T. Arima, S. Wakimoto, M. Takeda, K. Kakurai, and K. Kohn, Phys. Rev. Lett. **103**, 077204 (2009).
[7] M. Fukunaga, Y. Sakamoto, H. Kimura, and Y. Noda, J. Phys. Soc. Jpn. **80**, 014705 (2010).
[8] S. Park, Y. J. Choi, C. L. Zhang, and S. W. Cheong, Phys. Rev. Lett. **98**, 057601 (2007).
[9] K. Taniguchi, N. Abe, T. Takenobu, Y. Iwasa, and T. Arima, Phys. Rev. Lett. **97**, 097203 (2006).
[10] H. Katsura, N. Nagaosa, and A. V. Balatsky, Phys. Rev. Lett. **95**, 057205 (2005).
[11] S. Seki, Y. Yamasaki, M. Soda, M. Matsuura, K. Hirota, and Y. Tokura, Phys. Rev. Lett. **100**, 127201 (2008).
[12] K. Taniguchi, N. Abe, H. Umetsu, H. A. Katori, and T. Arima, Phys. Rev. Lett. **101**, 207205 (2008).
[13] M. Matsubara, S. Manz, M. Mochizuki, T. Kubacka, A. Iyama, N. Aliouane, T. Kimura, S. L. Johnson, D. Meier, and M. Fiebig, Science **348**, 1112 (2015).
[14] M. Mochizuki and N. Furukawa, Phys. Rev. Lett. **105**, 187601 (2010).
[15] I. E. Chupis and H. A. Kovtun, Appl. Phys. Lett. **103**, 182901 (2013).
[16] M. Mochizuki, Phys. Rev. B **92**, 224412 (2015).
[17] Y. Yamasaki, S. Miyasaka, Y. Kaneko, J. P. He, T. Arima, and Y. Tokura, Phys. Rev. Lett. **96**, 207204 (2006).
[18] K. Taniguchi, N. Abe, S. Ohtani, H. Umetsu, and T.-h. Arima, Appl. Phys. Express **1**, 031301 (2008).
[19] Y. J. Choi, J. Okamoto, D. J. Huang, K. S. Chao, H. J. Lin, C. T. Chen, M. Veenendaal, T. A. Kaplan, and S. W. Cheong, Phys. Rev. Lett. **102**, 067601 (2009).
[20] H. Mitamura, T. Sakakibara, H. Nakamura, T. Kimura, and K. Kindo, J. Phys. Soc. Jpn. **81**, 054705 (2012).
[21] R. D. Johnson, C. Mazzoli, S. R. Bland, C. H. Du, and P. D. Hatton, Phys. Rev. B **83**, 054438 (2011).
[22] H. Nojiri, S. Yoshii, M. Yasui, K. Okada, M. Matsuda, J. S. Jung, T. Kimura, L. Santodonato, G. E. Granroth, K. A. Ross, J. P. Carlo, and B. D. Gaulin, Phys. Rev. Lett. **106**, 237202 (2011).
[23] I. Urcelay-Olabarria, E. Ressouche, A. A. Mukhin, V. Y. Ivanov, A. M. Kadomtseva, Y. F. Popov, G. P. Vorob'ev, A. M. Balbashov, J. L. García-Muñoz, and V. Skumryev, Phys. Rev. B **90**, 024408 (2014).
[24] N. Abe, K. Taniguchi, S. Ohtani, T. Takenobu, Y. Iwasa, and T. Arima, Phys. Rev. Lett. **99**, 227206 (2007).
[25] K. Taniguchi, N. Abe, S. Ohtani, and T. Arima, Phys. Rev. Lett. **102**, 147201 (2009).
[26] R. Chen, J. F. Wang, Z. W. Ouyang, Z. Z. He, S. M. Wang, L. Lin, J. M. Liu, C. L. Lu, Y. Liu, C. Dong, C. B. Liu, Z. C. Xia, A. Matsuo, Y. Kohama, and K. Kindo, Phys. Rev. B **98**, 184404 (2018).
[27] L. Yin, Z. W. Ouyang, J. F. Wang, X. Y. Yue, R. Chen, Z. Z. He, Z. X. Wang, Z. C. Xia, and Y. Liu, Phys. Rev. B **99**, 134434 (2019).
[28] Z. W. Ouyang, Y. C. Sun, J. F. Wang, X. Y. Yue, R. Chen, Z. X. Wang, Z. Z. He, Z. C. Xia, Y. Liu, and G. H. Rao, Phys. Rev. B **97**, 144406 (2018).
[29] Z. He, J.-I. Yamaura, Y. Ueda, and W. Cheng, J. Solid State Chem. **182**, 2526 (2009).
[30] See Supplemental Material at http://link.aps.org/supplemental/10.1103/PhysRevB.100.140403 for more details of the electric-polarization switches in an applied magnetic field.
[31] E. Ascher, H. Rieder, H. Schmid, and H. Stössel, J. Appl. Phys. **37**, 1404 (1966).
[32] Y. J. Liu, J. F. Wang, Z. Z. He, C. L. Lu, Z. C. Xia, Z. W. Ouyang, C. B. Liu, R. Chen, A. Matsuo, Y. Kohama, K. Kindo, and M. Tokunaga, Phys. Rev. B **97**, 174429 (2018).
[33] F. Kagawa, M. Mochizuki, Y. Onose, H. Murakawa, Y. Kaneko, N. Furukawa, and Y. Tokura, Phys. Rev. Lett. **102**, 057604 (2009).
[34] N. Abe, K. Taniguchi, S. Ohtani, H. Umetsu, and T. Arima, Phys. Rev. B **80**, 020402 (2009).
[35] N. Aliouane, D. N. Argyriou, J. Strempfer, I. Zegkinoglou, S. Landsgesell, and M. v. Zimmermann, Phys. Rev. B **73**, 020102 (2006).
[36] K. Yoo, B. Koteswararao, J. Kang, A. Shahee, W. Nam, F. F. Balakirev, V. S. Zapf, N. Harrison, A. Guda, N. Ter-Oganessian, and K. H. Kim, npj Quantum Mater. **3**, 45 (2018).
[37] W. H. Ji, Y. C. Sun, C. M. N. Kumar, C. Li, S. Nandi, W. T. Jin, Y. Su, X. Sun, Y. Lee, B. Harmon, L. Ke, Z. W. Ouyang, Y. Xiao, and Th. Brückel, arXiv:1905.06282 [Phys. Rev. B (to be published)].
[38] S. Kimura, K. Kakihata, Y. Sawada, K. Watanabe, M. Matsumoto, M. Hagiwara, and H. Tanaka, Nat. Commun. **7**, 12822 (2016); Phys. Rev. B **95**, 184420 (2017).